Review

Bioimaging Based on Nucleic Acid Nanostructures

HAN Lin[1,2#], WANG Yuang[1,2#], TANG Wantao[1,2], LIU Jianbing[2]✉ and DING Baoquan[1,2]✉

Received February 11, 2021
Accepted March 15, 2021

Nucleic acid nanostructures with structural programmability, spatial addressability and excellent biocompatibility have drawn much attention in various biomedical applications, such as bioimaging, biosensing and drug delivery. In this review, we summarize the recent research progress in the field of bioimaging based on nucleic acid nanostructures with different imaging models, including fluorescent imaging(FI), magnetic resonance imaging(MRI), photoacoustic imaging(PAI) and positron emission tomography/computed tomography(PET/CT) imaging. We also discuss the remaining challenges and further opportunities involved in the bioimaging research based on nucleic acid nanostructures.

Keywords Nucleic acid nanostructure; DNA self-assembly; Bioimaging; Multimodal imaging

1 Introduction

Biomedical imaging technologies, such as fluorescent imaging(FI), magnetic resonance imaging(MRI), photoacoustic imaging(PAI) and positron emission tomography/computed tomography(PET/CT) imaging have been developed rapidly in recent years. Fast and efficient bioimaging systems with the subcellular resolution are urgently demanded in diagnosis and therapy. Imaging reagents, such as organic fluorescent probe, quantum dot(QD) and contrast agent, are widely employed in bioimaging systems. The successful loading and efficient delivery of these imaging reagents into the target region is the first critical step in precise diagnosis and therapy. Various delivery systems have been developed, such as polymers, dendrimers and inorganic nanoparticles[1—3]. Considering the possible cytotoxicity and immune response induced by these exogenous carriers[4,5], much attention has been drawn to the construction of biocompatible vectors for targeted bioimaging.

Biological macromolecules, such as nucleic acid, protein and polysaccharides are excellent materials for delivery research due to their superior biocompatibility. Nucleic acid, as a carrier of genetic information, has also attracted much attention to fabricate the biocompatible nucleic acid nanostructures. In the early 1980s, Seeman *et al.*[6—8] proposed that nucleic acid could be applied as the building blocks to assemble nanoscale architectures through classic Watson-Crick base pairing [Fig.1(A)]. In 2005, Turberfield and co-workers[9] fabricated a three-dimensional(3D) tetrahedral nanostructure based on four rationally designed oligonucleotides[Fig.1(B)]. Subsequently, a series of other polyhedral nucleic acid nanostructures, such as bipyramid[10], octahedra[11], and dodecahedron and buckyball[12] have been invented. In 2006, Rothemund[13] opened up a new window for the construction of a novel kind of DNA nanostructure, named DNA origami[Fig.1(C)], based on a long single-stranded DNA(scaffold) folded by multiple short oligonucleotides(staple strands). Besides the strands hybridization strategy, rolling circle amplification(RCA) has also been exploited to prepare DNA nanoflower and hydrogel[Fig.1(D)][14,15]. Until now, various nucleic acid nanostructures with rational designs have sprung up to enrich the big family of nucleic acid self-assembly[16—24].

Due to structural programmability, spatial addressability and excellent biocompatibility, nucleic acid nanostructures have been widely developed for biomedical applications, such as bioimaging[25—29], biosensing and drug delivery[30—53].

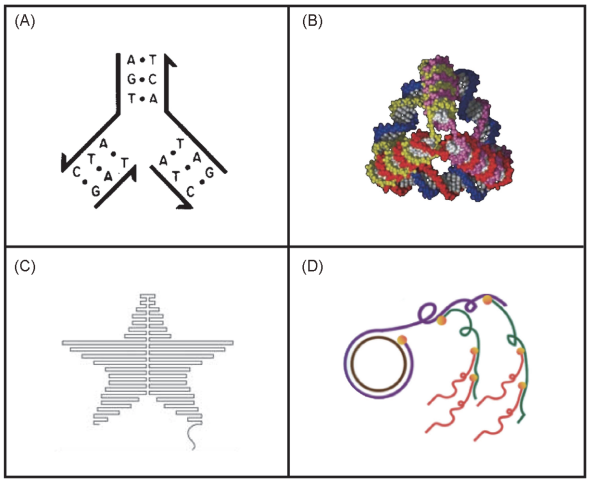

Fig.1 Examples of nucleic acid nanostructures
(A) DNA assembled junction[6]. Copyright 1982, Elsevier; (B) DNA tetrahedron[9]. Copyright 2005, American Association for the Advancement of Science; (C) DNA origami[13]. Copyright 2006, Nature Publishing Group; (D) DNA nanostructures based on rolling circle amplification(RCA)[14]. Copyright 2017, American Chemical Society.

✉ LIU Jianbing
liujb@nanoctr.cn
✉ DING Baoquan
dingbq@nanoctr.cn
# These authors contributed equally to this work.
1. School of Materials Science and Engineering, Henan Institute of Advanced Technology, Zhengzhou University, Zhengzhou 450001, P. R. China;
2. CAS Key Laboratory of Nanosystem and Hierarchical Fabrication, CAS Center for Excellence in Nanoscience, National Center for Nanoscience and Technology, Beijing 100190, P. R. China

https://doi.org/10.1007/s40242-021-1055-0

Multiple functional groups(such as imaging reagents and targeting ligands) modified oligonucleotides can be precisely arranged by the nucleic acid nanostructures through hybridization for efficient loading and targeted delivery. Due to the excellent biocompatibility, nucleic acid nanostructures hold great promise as efficient carriers for bioimaging reagents.

2 Fluorescent Imaging Based on Nucleic Acid Nanostructures

Fluorescent imaging(FI) is a powerful strategy to visualize the target under subcellular resolution. Various fluorescent probes can be covalently conjugated with the DNA oligonucleotides and then attached to the nucleic acid nanostructures through hybridization. DNA hydrogel assembled from branched DNA junctions is widely employed for biomedical applications. Tan and co-workers[54] reported the synthesis and characterization of size-controllable and stimuli-responsive DNA nanohydrogel for effective cellular imaging and targeted gene regulation [Fig.2(A)]. This aptamer modified DNA nanohydrogel achieved an evident cellular uptake in target A549 cells, which was tracked through the fluorescent signal of the labeled TAMRA probe. This kind of DNA nanohydrogel with target ability is promising for bioimaging and drug delivery.

The 3D polyhedral nucleic acid nanostructures, such as DNA tetrahedron, were extensively studied for subcellular bioimaging. Tian and co-workers[55] designed and fabricated a mitochondria-targeted DNA nanoprobe based on DNA tetrahedron for real-time subcellular imaging and simultaneous quantification of Ca^{2+} and pH[Fig.2(B)]. The Ca^{2+} fluorescent probe(CD@CaL), pH-responsive dye(FITC) and mitochondria-targeted molecule(TPP) were simultaneously assembled in the DNA tetrahedron with an inner-reference dye(AF660). This mitochondria-targeted nanoprobe demonstrated a high spatial bioimaging resolution with a long-term fluorescent. Moreover, Li and co-workers[56] reported a lysosome-recognizing framework nucleic acid nanodevice for subcellular imaging based on DNA logic operations[Fig.2(C)]. The ATP-binding aptamer and i-motif were co-assembled into a DNA triangular prism as the

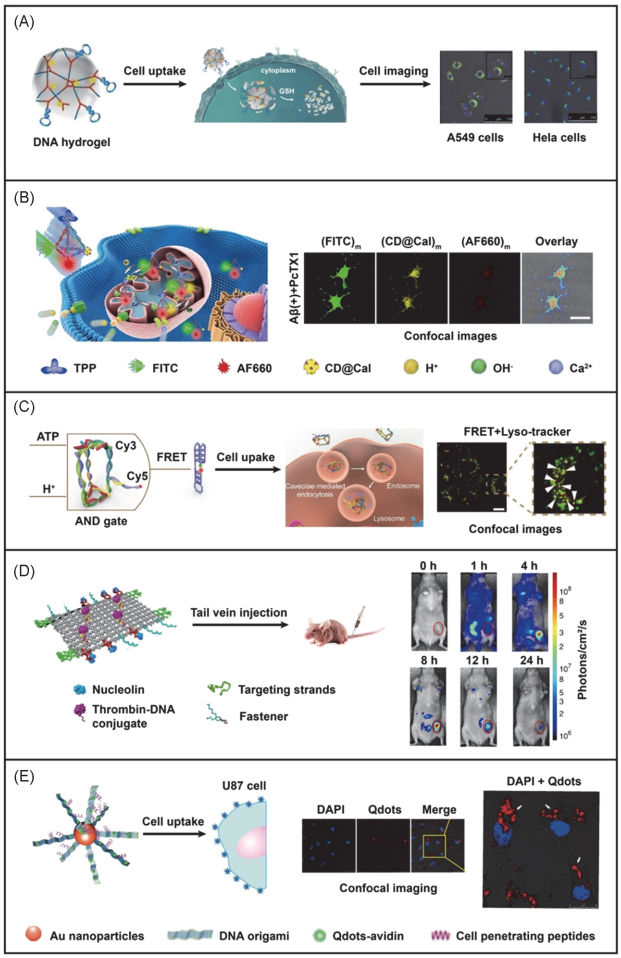

Fig.2 Fluorescent imaging(FI) based on nucleic acid nanostructures

(A) A DNA nanohydrogel for cellular FI[54]. Copyright 2015, American Chemical Society; (B) a DNA tetrahedron based nanoprobe for cellular FI[55]. Copyright 2018, American Chemical Society; (C) a framework nucleic acid nanodevice for cellular FI[56]. Copyright 2019, American Chemical Society; (D) a DNA origami-based nanorobot for FI *in vivo*[53]. Copyright 2018, Nature Publishing Group; (E) a 3D superstructure based on DNA origami and gold nanoparticles(AuNPs) for cellular FI[57]. Copyright 2015, Wiley.

https://doi.org/10.1007/s40242-021-1055-0

logic-controlling units. The structural change of the DNA nanodevice depended on the folding of ATP-binding aptamer and i-motif, which was triggered by the high concentration of ATP and low pH value in the lysosome. This DNA nanodevice with an AND logic gate(ATP and H^+) achieved a sensitive detection of ATP and pH, which would contribute to the efficient diagnosis.

DNA origami can be folded into tailored nanostructures to load various fluorescent dyes for bioimaging. Ding and co-workers[53] constructed an intelligent DNA nanorobot programmed to deliver thrombin specifically to the tumor-associated blood vessels and result in intravascular thrombosis[Fig.2(D)]. This DNA nanorobot was constructed by rolling up a square origami into a tubular nanostructure. It could load the thrombin in its inner cavity and expose it in the presence of nucleolin specifically expressed on tumor-associated endothelial cells. To visualize the targeted delivery, multiple Cy5.5-labeled oligonucleotides were introduced into the DNA nanorobot through DNA hybridization in the central region of the DNA origami. After the intravenous injection with the Cy5.5-labeled DNA nanorobot, a maximal accumulation in the tumor site was observed at 8 h after the injection. The aptamer-conjugated DNA nanorobot demonstrated a targeted delivery *in vivo* and resulted in tumor necrosis and tumor growth inhibition.

Rolling circle amplification is a promising strategy to construct nanoflower for the loading of imaging reagents. Song and co-workers[57] developed a novel 3D gold-DNA hybrid nanostructure by *in-situ* growth and origami folding of DNA on gold nanoparticles(AuNPs) for bioimaging and drug delivery[Fig.2(E)]. AuNPs were first modified with the thiolated DNA primer for *in-situ* RCA on the surface. The obtained multiple long single-stranded DNAs were then folded by the staple strands to construct DNA origami. This 3D gold-DNA hybrid nanostructure could be easily modified with QD through avidin-biotin binding. With the attachment of cell-penetrating peptides, the QD modified nanoplatform demonstrated efficient cellular uptake in U87 MG cells detected by confocal imaging.

3 Magnetic Resonance Imaging Based on Nucleic Acid Nanostructures

Magnetic resonance imaging(MRI), as a noninvasive detection strategy, is widely employed in clinical diagnosis and therapy. Magnetic resonance contrast agents are often used to obtain the enhanced imaging effect. Various nucleic acid nanostructures have been successfully developed to load the magnetic resonance contrast agents for targeted and efficient MRI *in vivo*.

Ding and co-workers[58] developed a versatile DNA bipyramid nanostructure into a tumor-targeted and dual-modal nanoprobe for *in vivo* imaging[Fig.3(A)]. The magnetic resonance contrast agent(gadolinium chelates Gd-DOTA) and fluorescent dye(Dylight800) were conjugated on the DNA oligonucleotides and precisely arranged on the DNA bipyramid nanostructure with nanometer spatial control. After the modification with the tumor-targeting group(anti-EGFR aptamer) and protective PEG-Lysine copolymer, the dual-modal nanoprobe demonstrated enhanced serum stability. It achieved a targeted co-delivery of magnetic resonance contrast agent and a fluorescent dye into the triple-negative breast tumor *in vivo*. This stabilized dual-modal imaging nanoplatform holds the potential for bioimaging in the clinic.

Yang and co-workers[59] reported a novel strategy to construct a DNA-Mn hybrid nanoflower for MRI[Fig.3(B)]. The paramagnetic Mn^{2+} was included in the RCA system to function as the co-factor of DNA polymerase. The DNA-Mn hybrid nanoflower was fabricated through the enzymatic biomineralization during the RCA process. Owing to the aptamer sequences encoded in the circle template, the constructed MRI nanoplatform demonstrated efficient cellular uptake and tumor targeting effect. This nanoplatform elicited

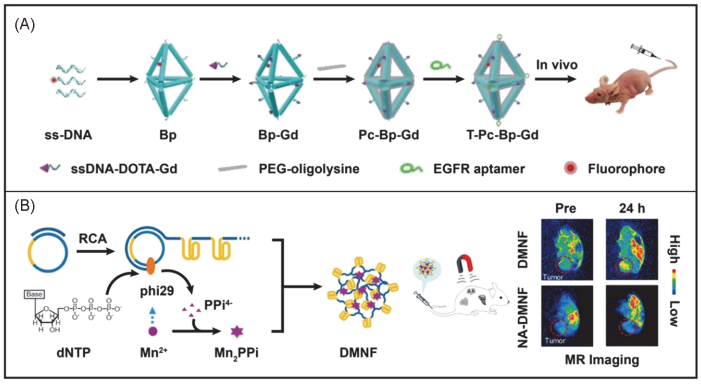

Fig.3 Magnetic resonance imaging(MRI) based on nucleic acid nanostructures

(A) A dual-modal nanoprobe based on DNA bipyramid nanostructure for MRI and FI *in vivo*[58]. Copyright 2020, American Chemical Society; (B) a nanoflower based on Mn^{2+} for MRI *in vivo*[59]. Copyright 2021, Elsevier.

https://doi.org/10.1007/s40242-021-1055-0

enhanced T_1-weighted MRI effect in tumor site and high spatial resolution imaging of kidneys and liver. This kind of DNA-metal hybrid nanosystem is facile to be scaled up, which is advantageous for future biomedical applications.

4 Photoacoustic Imaging Based on Nucleic Acid Nanostructures

Photoacoustic imaging(PAI) relies on the combination between optical excitation and ultrasonic detection. In contrast to FI, PAI possesses a greater penetration depth(cm *vs*. mm), which is critical for the bioimaging in deep tissues. To enhance the imaging resolution, various PA probes have been developed.

Lu and co-workers[60] reported a DNA aptamer-based selective and activatable PA probe for *in vivo* bioimaging [Fig.4(A)]. A near-infrared fluorophore/quencher pair(IRDye 800CW/IRDye QC-1) was pulled together through the hybridization of the DNA duplex. The DNA aptamer-based PA probe elicited an apparent change of the PA signal ratio at 780/725 nm after the addition of the target(thrombin) *in vivo*. This activatable PA probe realized the targeted PAI and can be developed into a general strategy for bioimaging and biosensing.

Tian and co-workers[61] developed a PAI agent by self-assembling gold nanorod onto the triangular DNA origami nanostructure[Fig.4(B)]. The DNA modified gold nanorod could be precisely organized on the surface of triangular DNA origami through DNA hybridization. After the intravenous injection, the gold/DNA hybrid nanoplatform achieved a better tumor accumulation with a deeper penetration at the tumor site than the free gold nanorod. Simultaneously, the gold/DNA hybrid nanoplatform could respond to NIR irradiation for photothermal therapy. This work provided a simple and effective strategy for the combination of PAI and photothermal therapy *in vivo*.

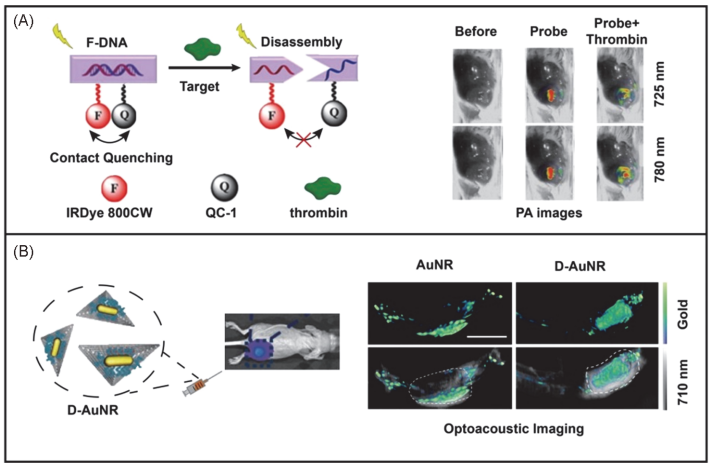

Fig.4 Photoacoustic imaging(PAI) based on nucleic acid nanostructures

(A) A PA probe based on DNA aptamer for PAI *in vivo*[60]. Copyright 2017, American Chemical Society; (B) a PA probe based on DNA origami and gold nanorod for PAI *in vivo*[61]. Copyright 2016, Wiley.

5 PET/CT Imaging Based on Nucleic Acid Nanostructures

PET/CT imaging, as a rapidly developed imaging technology, has been widely employed in the clinic. Various radionuclides, such as ^{68}Ga, ^{89}Zr and ^{64}Cu have been optimized and loaded by multifunctional nucleic acid nanostructures to obtain the enhanced imaging resolution and detection depth *in vivo*.

Virta and co-workers[62] synthesized a ^{68}Ga modified anti-microRNA-21 to load a bis(phosphonate) conjugated microRNA-21 for bone targeting and PET imaging *in vivo* [Fig.5(A)]. The ^{68}Ga chelate(^{68}Ga-NOTA) was conjugated on the 3′ terminal of anti-microRNA-21. The whole-body biodistribution of this modified RNA duplex was monitored by the PET imaging. After the intravenous administration, an increased bone accumulation was observed by gamma counting of excised tissues. This functionalized RNA duplex provided a simple and efficient imaging platform for bone targeting.

Fan and co-workers[63] reported a multiple-armed DNA tetrahedral nanostructure with the modification of radioactive isotope ^{99m}Tc and NIR emitter Dylight 755 for dual-modal imaging *in vivo*[Fig.5(B)]. The single-photon emission computed tomography(SPECT) imaging was performed by radioactive isotope ^{99m}Tc. After the conjugation of the tumor-targeting folic acid on the prescribed positions, this multifunctional DNA nanoplatform realized noninvasive tumor-targeting imaging *in vivo* by using both fluorescent and SPECT imaging modalities.

Cai and co-workers[64] developed an aptamer-conjugated and ^{89}Zr-radiolabeled framework nucleic acid for the repair of

https://doi.org/10.1007/s40242-021-1055-0

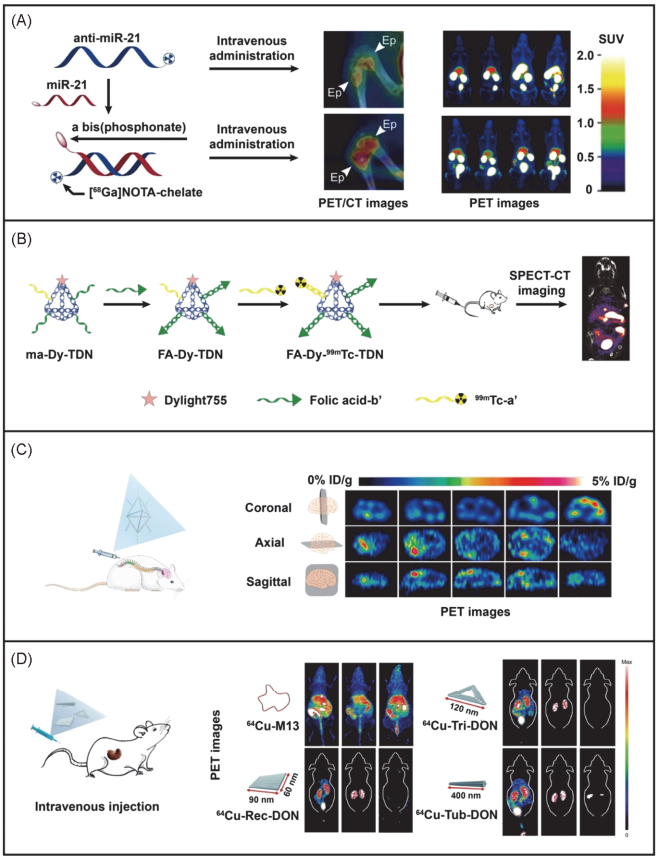

Fig.5 PET/CT imaging based on nucleic acid nanostructures

(A) A probe based on anti-microRNA-21/microRNA-21 for PET/CT imaging *in vivo*[62]. Copyright 2016, American Chemical Society; (B) a probe based on DNA tetrahedron for SPECT-CT imaging *in vivo*[63]. Copyright 2016, American Chemical Society; (C) a probe based on framework nucleic acid for PET imaging *in vivo*[64]. Copyright 2019, American Chemical Society; (D) a probe based on DNA origami for PET imaging *in vivo*[65]. Copyright 2018, Nature Publishing Group.

cerebral ischemia-reperfusion injury[Fig.5(C)]. After the intrathecal injection, the aptamer(anti-complement component 5a, anti-C5a) loaded framework nucleic acid could specifically recognize the C5a and selectively reduce C5a-mediated neurotoxicity. The PET imaging based on ^{89}Zr-radiolabeled single-stranded oligonucleotides revealed that the nanoplatform spread out in the ischemic penumbra. Moreover, Cai and co-workers[65] constructed ^{64}Cu-labelled DNA origami nanostructures to alleviate acute kidney injury[Fig.5(D)]. The ^{64}Cu chelate(^{64}Cu-NOTA) was included through conjugation on the single-stranded oligonucleotides. After the intravenous injection, the biodistribution resulted by PET imaging revealed that the DNA origami preferentially accumulated in the kidney of the mice with rhabdomyolysis-induced acute kidney injury. Interestingly, the accumulated DNA origami showed renal-protective activity. This work provided a novel solution to the treatment of acute kidney injury by DNA nanostructures.

6 Conclusions and Future Perspectives

Impressive progress has been achieved by using nucleic acid nanostructures as the carrier for bioimaging. In this review, we summarized the recent developments in the field of nucleic acid nanostructures assisted bioimaging, including FI, MRI, PAI and PET/CT imaging. Spatially addressable nucleic acid nanostructures can be functionalized with multiple imaging reagents through covalent conjugation or nucleic acid hybridization. After the modification with active targeting groups, the nucleic acid nanostructures can transport the imaging probes to the target tissues and organs and achieve a subcellular imaging resolution. This biocompatible and targeted bioimaging strategy based on nucleic acid nanostructures can be widely employed in diagnosis and therapy. Different types of imaging probes can be delivered together to realize multimodal imaging. In addition, the combination of information technology methods can improve the image processing and pattern recognition to achieve better contrast, resolution, sensitivity and signal-to-noise ratio. Some critical issues about the practical applications of this bioimaging system based on nucleic acid nanostructures still need to be properly addressed. The degradation and possible immunogenicity of nucleic acid nanostructures should be taken into consideration. Fortunately, chemical modification and rational sequence design are promising solutions to mitigate these risks. Another concern is the mass-production

https://doi.org/10.1007/s40242-021-1055-0

of DNA nanostructures at a low cost, which is critical for broad applications in clinics. Despite the above-mentioned challenges, we are expecting this tailored and precise bioimaging system based on nucleic acid nanostructures to play a more important role in pre-clinical and clinical theranostics.

Acknowledgements

This work was supported by the National Natural Science Foundation of China(Nos.22025201, 22077023 and 21721002), the National Basic Research Program of China(Nos.2016YFA0201601 and 2018YFA0208900), the Fund of the Beijing Municipal Science & Technology Commission, China (No.Z191100004819008), the Strategic Priority Research Program of Chinese Academy of Sciences(No.XDB36000000), the Key Research Program of Frontier Sciences of CAS(No.QYZDB-SSW-SLH029), and the CAS Interdisciplinary Innovation Team, Youth Innovation Promotion Association CAS and K. C. Wong Education Foundation(No.GJTD-2018-03).

Conflicts of Interest

The authors declare no conflicts of interest.

References

[1] Erathodiyil N., Ying J. Y., *Acc. Chem. Res.*, **2011**, *44*, 925
[2] Wolfbeis O. S., *Chem. Soc. Rev.*, **2015**, *44*, 4743
[3] Cheng H.-B., Li Y., Tang B. Z., Yoon J., *Chem. Soc. Rev.*, **2020**, *49*, 21
[4] Lim E. K., Kim T., Paik S., Haam S., Huh Y. M., Lee K., *Chem. Rev.*, **2015**, *115*, 327
[5] Lv H., Zhang S., Wang B., Cui S., Yan J., *J. Control. Release*, **2006**, *114*, 100
[6] Seeman N. C., *J. Theor. Biol.*, **1982**, *99*, 237
[7] Kallenbach N. R., Ma R.-I., Seeman N. C., *Nature*, **1983**, *305*, 829
[8] Chen J., Seeman N. C., *Nature*, **1991**, *350*, 631
[9] Goodman R. P., Schaap I. A., Tardin C. F., Erben C. M., Berry R. M., Schmidt C. F., Turberfield A. J., *Science*, **2005**, *310*, 1661
[10] Erben C. M., Goodman R. P., Turberfield A. J., *J. Am. Chem. Soc.*, **2007**, *129*, 6992
[11] He Y., Su M., Fang P.-A., Zhang C., Ribbe A. E., Jiang W., Mao C., *Angew. Chem. Int. Ed.*, **2010**, *49*, 748
[12] He Y., Ye T., Su M., Zhang C., Ribbe A. E., Jiang W., Mao C., *Nature*, **2008**, *452*, 198
[13] Rothemund P. W., *Nature*, **2006**, *440*, 297
[14] Wang D., Hu Y., Liu P., Luo D., *Acc. Chem. Res.*, **2017**, *50*, 733
[15] Ali M. M., Li F., Zhang Z., Zhang K., Kang D.-K., Ankrum J. A., Le X. C., Zhao W., *Chem. Soc. Rev.*, **2014**, *43*, 3324
[16] Li Y., Tseng Y. D., Kwon S. Y., d'Espaux L., Bunch J. S., McEuen P. L., Luo D., *Nat. Mater.*, **2003**, *3*, 38
[17] Douglas S. M., Dietz H., Liedl T., Högberg B., Graf F., Shih W. M., *Nature*, **2009**, *459*, 414
[18] Han D., Pal S., Nangreave J., Deng Z., Liu Y., Yan H., *Science*, **2011**, *332*, 342
[19] Benson E., Mohammed A., Gardell J., Masich S., Czeizler E., Orponen P., Hogberg B., *Nature*, **2015**, *523*, 441
[20] Ong L. L., Hanikel N., Yaghi O. K., Grun C., Strauss M. T., Bron P., Lai-Kee-Him J., Schueder F., Wang B., Wang P., Kishi J. Y., Myhrvold C., Zhu A., Jungmann R., Bellot G., Ke Y., Yin P., *Nature*, **2017**, *552*, 72
[21] Song J., Li Z., Wang P., Meyer T., Mao C., Ke Y., *Science*, **2017**, *357*, eaan3377
[22] Tikhomirov G., Petersen P., Qian L., *Nature*, **2017**, *552*, 67
[23] Wagenbauer K. F., Sigl C., Dietz H., *Nature*, **2017**, *552*, 78
[24] Dong Y., Yao C., Zhu Y., Yang L., Luo D., Yang D., *Chem. Rev.*, **2020**, *120*, 9420
[25] Bhatia D., Surana S., Chakraborty S., Koushika S. P., Krishnan Y., *Nat. Commun.*, **2011**, *2*, 339
[26] Hu R., Zhang X.-B., Kong R.-M., Zhao X.-H., Jiang J., Tan W., *J. Mater. Chem.*, **2011**, *21*, 16323
[27] Meng H.-M., Liu H., Kuai H., Peng R., Mo L., Zhang X.-B., *Chem. Soc. Rev.*, **2016**, *45*, 2583
[28] Bi S., Yue S., Zhang S., *Chem. Soc. Rev.*, **2017**, *46*, 4281
[29] Tam D. Y., Dai Z., Chan M. S., Liu L. S., Cheung M. C., Bolze F., Tin C., Lo P. K., *Angew. Chem. Int. Ed.*, **2016**, *55*, 164
[30] Schüller V. J., Heidegger S., Sandholzer N., Nickels P. C., Suhartha N. A., Endres S., Bourquin C., Liedl T., *ACS Nano*, **2011**, *5*, 9696
[31] Douglas S. M., Bachelet I., Church G. M., *Science*, **2012**, *335*, 831
[32] Jiang Q., Song C., Nangreave J., Liu X., Lin L., Qiu D., Wang Z.-G., Zou G., Liang X., Yan H., Ding B., *J. Am. Chem. Soc.*, **2012**, *134*, 13396
[33] Lee H., Lytton-Jean A. K., Chen Y., Love K. T., Park A. I., Karagiannis E. D., Sehgal A., Querbes W., Zurenko C. S., Jayaraman M., Peng C. G., Charisse K., Borodovsky A., Manoharan M., Donahoe J. S., Truelove J., Nahrendorf M., Langer R., Anderson D. G., *Nat. Nanotechnol.*, **2012**, *7*, 389
[34] Lee J. B., Hong J., Bonner D. K., Poon Z., Hammond P. T., *Nat. Mater.*, **2012**, *11*, 316
[35] Liang H., Zhang X.-B., Lv Y., Gong L., Wang R., Zhu X., Yang R., Tan W., *Acc. Chem. Res.*, **2014**, *47*, 1891
[36] Pei H., Zuo X., Zhu D., Huang Q., Fan C., *Acc. Chem. Res.*, **2014**, *47*, 550
[37] Sun W., Ji W., Hall J. M., Hu Q., Wang C., Beisel C. L., Gu Z., *Angew. Chem. Int. Ed.*, **2015**, *54*, 12029
[38] Bujold K. E., Hsu J. C. C., Sleiman H. F., *J. Am. Chem. Soc.*, **2016**, *138*, 14030
[39] Schaffert D. H., Okholm A. H., Sørensen R. S., Nielsen J. S., Tørring T., Rosen C. B., Kodal A. L. B., Mortensen M. R., Gothelf K. V., Kjems J., *Small*, **2016**, *12*, 2634
[40] Yang Y., Wang J., Shigematsu H., Xu W., Shih W. M., Rothman J. E., Lin C., *Nat. Chem.*, **2016**, *8*, 476
[41] Mou Q., Ma Y., Pan G., Xue B., Yan D., Zhang C., Zhu X., *Angew. Chem. Int. Ed.*, **2017**, *56*, 12528
[42] Rahman M. A., Wang P., Zhao Z., Wang D., Nannapaneni S., Zhang C., Chen Z., Griffith C. C., Hurwitz S. J., Chen Z. G., Ke Y., Shin D. M., *Angew. Chem. Int. Ed.*, **2017**, *56*, 16023
[43] Veetil A. T., Chakraborty K., Xiao K., Minter M. R., Sisodia S. S., Krishnan Y., *Nat. Nanotechnol.*, **2017**, *12*, 1183
[44] Bastings M. M. C., Anastassacos F. M., Ponnuswamy N., Leifer F. G., Cuneo G., Lin C., Ingber D. E., Ryu J. H., Shih W. M., *Nano Lett.*, **2018**, *18*, 3557
[45] Ding F., Mou Q., Ma Y., Pan G., Guo Y., Tong G., Choi C. H. J., Zhu X., Zhang C., *Angew. Chem. Int. Ed.*, **2018**, *57*, 3064
[46] Liu J., Song L., Liu S., Zhao S., Jiang Q., Ding B., *Angew. Chem. Int. Ed.*, **2018**, *57*, 15486
[47] Hu Q., Li H., Wang L., Gu H., Fan C., *Chem. Rev.*, **2019**, *119*, 6459
[48] Liu J., Wu T., Lu X., Wu X., Liu S., Zhao S., Xu X., Ding B., *J. Am. Chem. Soc.*, **2019**, *141*, 19032
[49] Mou Q., Ma Y., Ding F., Gao X., Yan D., Zhu X., Zhang C., *J. Am. Chem. Soc.*, **2019**, *141*, 6955
[50] Wu T., Liu J., Liu M., Liu S., Zhao S., Tian R., Wei D., Liu Y., Zhao Y., Xiao H., Ding B., *Angew. Chem. Int. Ed.*, **2019**, *58*, 14224
[51] Sun W., Wang J., Hu Q., Zhou X., Khademhosseini A., Gu Z., *Sci. Adv.*, **2020**, *6*, eaba2983
[52] Liu J., Lu X., Wu T., Wu X., Han L., Ding B., *Angew. Chem. Int. Ed.*, **2021**, *60*, 1853
[53] Li S., Jiang Q., Liu S., Zhang Y., Tian Y., Song C., Wang J., Zou Y., Anderson G. J., Han J. Y., Chang Y., Liu Y., Zhang C., Chen L., Zhou G., Nie G., Yan H., Ding B., Zhao Y., *Nat. Biotechnol.*, **2018**, *36*, 258
[54] Li J., Zheng C., Cansiz S., Wu C., Xu J., Cui C., Liu Y., Hou W., Wang Y., Zhang L., Teng I. T., Yang H. H., Tan W., *J. Am. Chem. Soc.*, **2015**, *137*, 1412
[55] Liu Z., Pei H., Zhang L., Tian Y., *ACS Nano*, **2018**, *12*, 12357
[56] Du Y., Peng P., Li T., *ACS Nano*, **2019**, *13*, 5778
[57] Yan J., Hu C., Wang P., Zhao B., Ouyang X., Zhou J., Liu R., He D., Fan C., Song S., *Angew. Chem. Int. Ed.*, **2015**, *54*, 2431
[58] Song L., Wang Z., Liu J., Wang T., Jiang Q., Ding B., *ACS Appl. Bio Mater.*, **2020**, *3*, 2854
[59] Zhao H., Lv J., Li F., Zhang Z., Zhang C., Gu Z., Yang D., *Biomaterials*, **2021**, *268*, 120591
[60] Zhang J., Smaga L. P., Satyavolu N. S. R., Chan J., Lu Y., *J. Am. Chem. Soc.*, **2017**, *139*, 17225
[61] Du Y., Jiang Q., Beziere N., Song L., Zhang Q., Peng D., Chi C., Yang X., Guo H., Diot G., Ntziachristos V., Ding B., Tian J., *Adv. Mater.*, **2016**, *28*, 10000
[62] Jadhav S., Käkelä M., Bourgery M., Rimpilä K., Liljenbäck H., Siitonen R., Mäkilä J., Laitala-Leinonen T., Poijärvi-Virta P., Lönnberg H., Roivainen A., Virta P., *Mol. Pharm.*, **2016**, *13*, 2588
[63] Jiang D., Sun Y., Li J., Li Q., Lv M., Zhu B., Tian T., Cheng D., Xia J., Zhang L., Wang L., Huang Q., Shi J., Fan C., *ACS Appl. Mater. Interfaces*, **2016**, *8*, 4378
[64] Li S., Jiang D., Rosenkrans Z. T., Barnhart T. E., Ehlerding E. B., Ni D., Engle J. W., Cai W., *Nano Lett.*, **2019**, *19*, 7334
[65] Jiang D., Ge Z., Im H. J., England C. G., Ni D., Hou J., Zhang L., Kutyreff C. J., Yan Y., Liu Y., Cho S. Y., Engle J. W., Shi J., Huang P., Fan C., Yan H., Cai W., *Nat. Biomed. Eng.*, **2018**, *2*, 865